# An overview of the current clinical status of optical imaging in head and neck cancer with a focus on Narrow Band imaging and fluorescence optical imaging

van Schaik, Jeroen; Halmos, György B.; Witjes, Max; Plaat, B.

*Published in:*
Oral Oncology

*DOI:*
10.1016/j.oraloncology.2021.105504

Oral Oncology 121 (2021) 105504

Contents lists available at ScienceDirect

Oral Oncology

journal homepage: www.elsevier.com/locate/oraloncology

# An overview of the current clinical status of optical imaging in head and neck cancer with a focus on Narrow Band imaging and fluorescence optical imaging

Jeroen E. van Schaik [a,*], Gyorgy B. Halmos [a], Max J.H. Witjes [b], Boudewijn E.C. Plaat [a]

[a] Department of Otorhinolaryngology, Head and Neck Surgery, University of Groningen, University Medical Center Groningen, Groningen, the Netherlands
[b] Department of Oral and Maxillofacial Surgery, University of Groningen, University Medical Center Groningen, the Netherlands

ARTICLE INFO

*Keywords:*
Head and neck squamous cell carcinoma
Molecular imaging
Optical imaging
Narrow band imaging
Surgical margins

ABSTRACT

Early and accurate identification of head and neck squamous cell carcinoma (HNSCC) is important to improve treatment outcomes and prognosis. New optical imaging techniques may assist in both the diagnostic process as well as in the operative setting by real-time visualization and delineation of tumor. Narrow Band Imaging (NBI) is an endoscopic technique that uses blue and green light to enhance mucosal and submucosal blood vessels, leading to better detection of (pre)malignant lesions showing aberrant blood vessel patterns. Fluorescence optical imaging makes use of near-infrared fluorescent agents to visualize and delineate HNSCC, resulting in fewer positive surgical margins. Targeted fluorescent agents, such as fluorophores conjugated to antibodies, show the most promising results. The aim of this review is: (1) to provide the clinical head and neck surgeon an overview of the current clinical status of various optical imaging techniques in head and neck cancer; (2) to provide an in-depth review of NBI and fluorescence optical imaging, as these techniques have the highest potential for clinical implementation; and (3) to describe future improvements and developments within the field of these two techniques.

## Introduction

Delay in diagnosis of head and neck squamous cell carcinoma (HNSCC) ultimately results in advanced stage tumors with poorer survival. Despite extensive treatments, this consequently leads to higher treatment-related morbidity [1]. Identification of early (pre)malignant lesions is generally recognized as essential in HNSCC. In the past decades, much attention has been devoted to developing optical techniques to detect lesions at an early stage and correctly diagnose suspicious lesions. Recent technological developments in optical imaging have enabled new possibilities for early detection, better classification, and intraoperative tumor margin delineation. The main advantage of optical techniques over conventional radiologic imaging techniques is the potential to detect superficial mucosal lesions before being visible on scans. As conventional imaging techniques cannot be used intraoperatively, optical techniques for visualization of tumor borders and identification of tumor tissue during surgery is desirable.

In this review we aim to provide a brief overview of current optical techniques with real-time applicability for the detection and optical visualization of HNSCC tumors intraoperatively. Moreover, Narrow Band Imaging (NBI) and near-infrared (NIR) fluorescence imaging will be discussed more extensively, since these techniques are gaining more interest in clinical use because they provide wide-field real-time visualization.

## Techniques with real-time applicability

New techniques with real-time applicability have been attempted in order to better detect or delineate primary HNSCC for the purpose of either mucosal or deep margin assessment during surgery (Fig. 1). Optical techniques can currently be divided into techniques that use surface or subsurface visualization of the target tissue, quantify optical properties or expose tissue characteristics by adding optical agents into the tissue [2,3]. The various optical imaging techniques function optimally within a certain range of the light spectrum. Wavelengths in the visible light spectrum (<650 nm) are absorbed by hemoglobin and absorption

* Corresponding author at: Department of Otorhinolaryngology, Head and Neck Surgery, University of Groningen, University Medical Center Groningen, Hanzeplein 1, 9700RB Groningen the Netherlands.
*E-mail address:* j.e.van.schaik@umcg.nl (J.E. van Schaik).

https://doi.org/10.1016/j.oraloncology.2021.105504
Received 16 June 2021; Received in revised form 25 July 2021; Accepted 18 August 2021
Available online 25 August 2021

by components such as water and lipids are within the infrared range (>900 nm) [4]. The optimal window for fluorescent dyes is therefore in the near infrared (NIR) spectrum (700–900 nm), in which light may travel up to millimeters rather than micrometers [5].

For tumor delineation and visualization there are several mucosal staining methods. ***Lugol's iodine solution*** stains normal mucosa brown but leaves dysplastic epithelium white or pink in color as a result of decreased glycogen in these tissues [6]. In the detection of oral SCC and dysplastic lesions an 88% sensitivity and 84% specificity were found and it was shown to reduce the incidence of dysplasia in mucosal surgical margins (Table 1) [7,8]. The low specificity can be attributed to areas with inflammation, hyperkeratosis and mucus, as these cause the tissue to remain unstained [8]. Lugol has not been applied widely due to its low specificity and limited applicability in the oral cavity, since it can

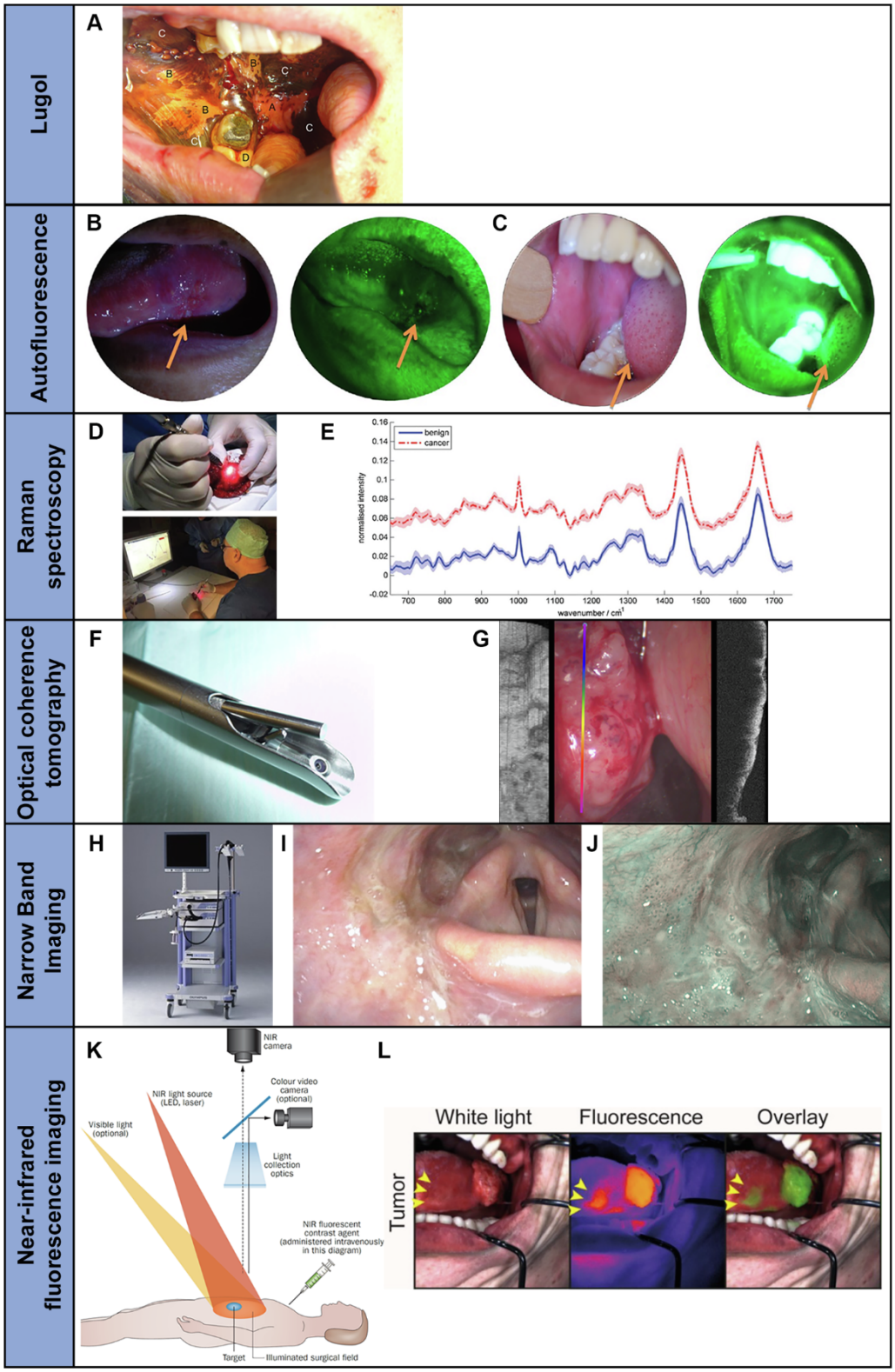


**Figure 1.** Overview of the setup and visual interpretation of the various techniques.**A)** Lugol: a) unstained squamous cell carcinoma in oral cavity, b) dysplastic areas, c) normal parakeratinized mucosa, d) normal orthokeratinized mucosa (reproduced from McMahon et al., by permission of Elsevier) [8]; Autofluorescence: **B)** oral cancer of the tongue with loss of fluorescence and **C)** normal tongue mucosa (reproduced from Huang et al., by permission of Elsevier) [91]; Raman spectroscopy: **D)** fiber needle probe setup (reproduced from Santos et al., by permission of STM) [28], **E)** visual depiction of benign and cancer tissue (reproduced from Lloyd et al., by permission of STM) [97]; Optical coherence tomography (OCT): **F)** OCT probe for examination (reproduced from Volgger et al., by permission of Wiley) [15], **G)** glottic carcinoma with an OCT-3D image left and OCT image on the right (reproduced from Englhard et al., by permission of Wiley) [95]; Narrow band imaging (NBI): **H)** Olympus NBI flexible scope setup [98], pharyngeal carcinoma shown using **I)** white light and **J)** NBI [42] (reproduced by permission of Olympus); Near-infrared fluorescence imaging: **K)** setup (reproduced from Vahrmeijer et al., by permission of Macmillan Published Limited) [5], **L)** white light, fluorescence and overlay images of a tongue cancer, the yellow arrows point towards a separate lesion detected using fluorescence (reproduced from Voskuil et al., CC by 4.0). [77].

**Table 1**
Sensitivity and specificity rate for each imaging technique per HNSCC site.

| Technique | Oral Cavity | | Oropharyx | | Hypopharynx | | Larynx | |
|---|---|---|---|---|---|---|---|---|
| | Sens | Spec | Sens | Spec | Sens | Spec | Sens | Spec |
| Lugol | 88[1] | 84[1] | – | – | – | – | – | – |
| Autofluorescence | 92–98[2] | 76–92[2] | – | – | – | – | 91*[3] | 84*[3] |
| Raman spectroscopy | 100[4] | 77–93[4] | – | – | 75[5] | 75[5] | 90[6] | 92[6] |
| OCT | 90–100[7] | 87–100[7] | – | – | – | – | 80–88[8] | 89–94[8] |
| Narrow Band Imaging | 76*[9] | 92*[9] | 76*[9] | 92*[9] | 82*[10] | 92*[10] | 90*[11] | 90*[11] |
| NIR fluorescence imaging | 97-100[‡12] | 74-91[‡12] | 91[~13] | 91[~13] | 91[~13] | 91[~13] | 91[~13] | 91[~13] |

**meta*-analysis; - no sensitivity and specificity rate found in literature for this site; [‡] using IRDye800CW; [~] using indocyanine green[90]; HNSCC: head and neck squamous cell carcinoma; OCT: optical coherence tomography; NIR: near-infrared; Sens: sensitivity; Spec: specificity. Sensitivity and specificity rates in percentage (%). [1][7]; [2][91,92]; [3][20]; [4][24,93]; [5][94]; [6][25]; [7][14,18]; [8][95,96]; [9][47]; [10][34]; [11][39]; [12][73,77]; [13][90].

only be used in non-keratinized epithelium. Moreover, in other HNSCC sites it poses the risk of aspiration into the airway [9]. ***Toluidine blue*** has an affinity for nucleic acids. As dysplastic and abnormal tissues have higher RNA and DNA content, they show more intense staining than healthy tissues [10]. A recent *meta*-analysis found only a 75% sensitivity and 60% specificity for the detection of oral lesions [11]. Toluidine blue therefore has, like Lugol, limited clinical benefits.

Although not strictly optical imaging, ***Intraoral ultrasound*** is a method that is increasingly used for determining the mucosal and deep resection margins of oral tongue SCC with promising results [12]. In a systematic review, eight out of ten studies showed a significant correlation between ultrasonographically measured and histologic tumor thickness. Best results are obtained in vivo and in two studies comparing with MRI, ultrasound was more precise. The results, however, need to be validated in prospective studies using the same methodology. A limiting factor for the application of ultrasound intraorally is the proximity of bone or salivary glands, which compromises the interpretation of the images. As ultrasound is not an optical imaging technique, it is not discussed further here.

***Optical coherence tomography (OCT)***, analogous to ultrasound, uses reflecting coherent light to make cross-sectional images of the underlying architecture in real-time with a penetration depth of 0.5–2 mm [13-15]. It is best used in the oral cavity due to its accessibility, where epithelial thickening may indicate malignancy [16]. In a healthy larynx it can identify the different layers; however, in laryngeal cancer the boundary of the basal membrane is lost and leads to unrecognizable structures, hampering identification and diagnosis [17]. In vivo sensitivity and specificity rates of 100% were found for the detection of oral SCC, compared to 93% and 69% for dysplastic lesions, respectively [18]. A limitation of OCT, however, is that it cannot differentiate between malignancy and inflammation [16]. OCT is still far from implementation in everyday clinical practice, as there is no classification to consistently diagnose lesions and since results need to be validated.

***Autofluorescence*** can be detected due to endogenous fluorophores, such as structural proteins. Most of the autofluorescence is emitted between 450 and 650 nm and disappears beyond 1500 nm [19]. The endogenous fluorophores appear in green when excited by ultraviolet light or visible light radiation of certain wavelengths [20,21]. Precancerous and malignant lesions appear as red-violet caused by an altered metabolism in tumor cells, less collagen in neoplastic lesions emitting fewer photons, and due to a loss of fluorescent signal resulting from epithelial thickening (blocking excitatory blue light) [20,22]. In a *meta*-analysis of oral lesions a 78% sensitivity and 48% specificity were found and autofluorescence had a lower area under the curve than regular clinical examination ($p = 0.0023$) [11]. The low specificity may be caused by interpretation errors of images due to variety in autofluorescence caused by scar formation, minimal amounts of blood, bacterial overgrowth and inflammation, limiting its clinical benefit compared to white light examination [21].

***Raman spectroscopy*** is based on the fact that photons are scattered at a different wavelength (up or down wavelength shift) due to energy loss while interacting with the vibrational modes of certain molecules (inelastic scattering) [23]. This shift in wavelength is measured and called the Raman scatter. In a pilot study, Raman spectroscopy was able to differentiate (pre)malignant oral lesions from normal tissue with a 100% sensitivity and 77% specificity [24]. In a small study of laryngeal biopsy specimens, a 90% sensitivity and 92% specificity was found for the detection of laryngeal SCC [25]. Although these results seem promising, analyzing an entire specimen may take up to several hours, in vivo accessibility is difficult as only rigid scopes can be used, and interpretation of results is more mathematical than visual. To analyze a specimen more quickly, the number of measurements could be reduced by sampling spectroscopy data only in specific areas of interest with a focus on spectral features associated with the presence of cancer cells (such as water content). In this manner, a 99% sensitivity and 92% specificity was found in the detection of tongue SCC, as tumor tissue had higher water content than healthy tissues [26]. Raman spectroscopy has not yet been developed for commercial applications and the first system for surgical guidance in head and neck tumors was expected to be ready for clinical trials in 2019 [27,28]. Due to the rather technical nature of spectroscopy and non-visual applications, including the interpretation of results, this does not fall within the scope of this review. Raman spectroscopy, as other spectroscopies such as inelastic reflectance spectroscopies, may, however, serve as an additional tool supporting visual observations since spectroscopic techniques have the capacity to provide quantitative measurements, whereas visual techniques are at best semi-quantitative.

From the above-described optical techniques, Narrow Band Imaging (NBI) and Fluorescence optical imaging are currently most widely and continuously studied in clinical trials by a multitude of academic centers, reflecting a higher possibility of adaptation into routine clinical use in the foreseeable future. We therefore focus the review more on these two techniques.

## NBI and fluorescence molecular optical imaging – Current clinical status

### *Narrow Band imaging*

In the development of cancer, the structure and organization of vasculature may change considerably due to angiogenesis, forming intraepithelial papillary capillary loops (IPCL) [29]. Enhanced visualization of these new abnormal blood vessels leads to increased and earlier detection of precancerous and cancerous lesions [30]. NBI is an endoscopic optical imaging technique that has gained increasing attention over the past two decades. Rather than using conventional white light, two narrow band filters of blue and green are used. These filters have a bandwidth of 30 nm with central wavelengths of 415 nm and 540 nm, respectively, which are maximally absorbed by hemoglobin [9]. As longer wavelengths of light penetrate more deeply into tissues due to scattering and absorption properties, the blue light at 415 nm enhances the visualization of superficial mucosal vascular patterns and the green

light at 540 nm enhances submucosal IPCLs [31]. The light is captured by a charge coupled device at the tip of the videoendoscope and the image is then reconstructed, displaying the superficial vessels in brown and submucosal vessels in cyan, increasing the contrast between vasculature and surrounding mucosa [30,32]. Positive NBI findings are generally described as well-demarcated brownish areas with scattered brown dots [33]. NBI seems to be a promising technique in the detection of laryngeal, pharyngeal and oral malignancies with an overall sensitivity of 89% and specificity of 96% and was found to perform better when combined with white light imaging (WLI) [33,34]. However, NBI (or comparable imaging techniques) is not considered standard of care yet, since evidence on the influence of NBI on clinical outcome or effect on health care costs has not yet been provided by large prospective studies or randomized controlled trials.

As vascular patterns associated with (pre)malignant lesions depend on the mucosa type, these alterations differ per HNSCC site and therefore different classifications are being used.

*NBI in detection of laryngeal lesions*

Laryngeal cancer is one of the most common types of HNSCC [35]. The most widely used classification for describing laryngeal lesions using NBI was described by Ni et al. (Fig. 2) [30]. They divided lesions into five types. Types I to III represent non-malignant lesions: type I) thin, oblique, and treelike/arborescent vessels without IPCLs; type II) enlarged diameter of oblique and arborescent vessels without IPCLs; type III) a white patch on the mucosa may, depending on its thickness, obscure the arborescent vessels, without IPCLs. Types IV and V indicate (pre)malignant lesions: type IV) IPCLs are visible as scattered, regular, small, and dark brown spots; type V) a: high density of irregular IPCLs that appear hollow, brownish and speckled and in various shapes, b: IPCLs are destroyed and appear 'woven' with tortuous and line-like shapes, c: uneven density and irregularly scattered brown speckles or tortuous shapes [30,36]. As there is no significant difference in sensitivity and specificity for a cut-off value for types IV and V combined or solely type V, a more recent classification described by the European Laryngological Society (ELS) might seem more applicable [37]. It describes benign conditions to show longitudinal vascular changes with increased number and density of blood vessels and changes of direction, while precancerous or cancerous lesions are characterized by their newly formed perpendicular blood vessels, recognized as dilated IPCLs [38].

In the largest and most recent *meta*-analysis of NBI in laryngeal cancer, a 90% sensitivity and 90% specificity were found for NBI, compared to 78% and 77% for WLI, respectively [39]. NBI showed excellent interrater reliability with an intraclass correlation coefficient of 0.91, in line with earlier findings concluding that NBI improves inter- and intraobserver agreement for both experienced and less-experienced observers [40]. As some lesions may cause difficulties in interpretation when strictly following classifications, lesion-specific clinical features should also be taken into account [41]. Caution should be taken when interpreting results on the accuracy of NBI, as these results are highly dependent on the experience of the observers, whether clinical information was available, and on the type of evaluated and included lesions. For instance, papillomas and post-treatment mucosa influences correct interpretation, as these lesions often appear with Ni type V vascular patterns [36,41,42]. In the ELS classification, the difficulty of discerning papillomas is overcome by describing HPV-related recurrent respiratory papillomatosis as vessel loops with a wide-angled turning point in a three-dimensional warty structure, compared to symmetrically arranged loops with a narrow-angled turning point for precancerous lesions [38].

*NBI in detection of lesions in the oral cavity, oropharynx and hypopharynx*

In the pharynx and oral cavity, three different types of epithelium can be found: type 1) keratinized thick stratified squamous; type 2a) nonkeratinized thin or 2b) very thick stratified squamous; type 3) pseudo-stratified ciliated columnar epithelium [43]. Consequently, the criteria described for laryngeal lesions cannot be applied. As the penetration depth of blue and green light is respectively 170 μm and 240 μm, this could limit the evaluation of some lesions in oral cavity and oropharyngeal subsites, where the mean mucosal thickness measures up to 1300 μm [44]. Consequently, the prevalence of brownish spots in early mucosal cancer was significantly higher in type 2a mucosa (floor of

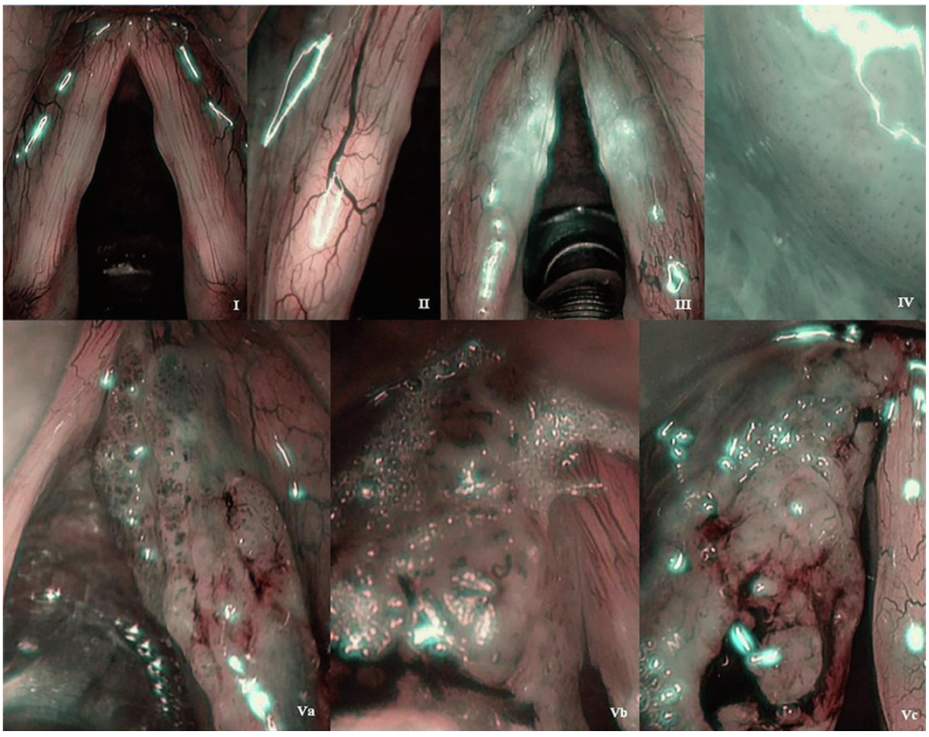


**Figure 2.** The NBI classification of laryngeal lesions as described by Ni et al. Reproduced from Zwakenberg et al., by permission of Wiley [40].

mouth, ventral tongue, soft palate, palatine tonsils, base of tongue, epiglottis and hypopharynx) compared to other types of mucosa in different subsites [43]. A widely used classification by Takano et al. was shown to perform significantly better than other classifications (Fig. 3) [45,46]. This classification divides findings into four types: type I) normal mucosa, regular brown dots, type II) IPCL pattern dilation and crossing, type III) IPCL pattern elongation and meandering, and type IV) IPCL pattern destruction and angiogenesis following a sequence of carcinogenesis progression [45]. In a *meta*-analysis a sensitivity of 76% and specificity of 92% were found for the detection of oral cavity and oropharyngeal dysplastic or malignant lesions using NBI [47]. Moreover, as leukoplakia may transform into malignancies in up to 18% and erythroplakia in up to 91% of the cases, increased detection rates of these precancerous lesions by NBI is beneficial [44]. Piazza et al. showed that the performance of NBI (sensitivity 89%, specificity 85%) was significantly superior to WLI (sensitivity 78%, specificity 73%) or conventional oral examination (sensitivity 51%, specificity 68%) [44].

*Detection of the primary tumor in neck metastasis of an unknown primary HNSCC*

SCC lymph node metastasis without any overt primary tumor, i.e. an unknown primary tumor (UPT), occurs in up to 4% of all HNSCC and is associated with a poor prognosis [48]. Conventional imaging techniques such as PET-CT, which has a 44% sensitivity and 97% specificity, may miss small superficial mucosal lesions [49]. A most recent technique, mucosectomy using an operation robot, adds transoral removal of lingual tonsils to palatine tonsillectomy, thereby increasing the detection rate of primary tumors [50]. However, this technique is invasive with a chance of complications and morbidity. NBI could overcome these limitations, and sensitivity rates of 74–91% and specificity rates of 86–95% have been reported [33,51]. Although detection rates may seem relatively low, it should be considered that these are found after a full clinical workup, sometimes even after biopsies and tonsillectomy [33]. Filauro et al. identified previously undetected lesions in 35% of patients using NBI, even after WLI endoscopy and CT, MRI or PET-CT [51]. As the lesions detected by NBI were generally small, they may still be removed by endoscopic resection, avoiding large field radiation and associated toxicity [33].

*NBI in detection of recurrences*

Radiotherapy or chemoradiotherapy cause changes to the mucosa which make identification of recurrent lesions more difficult. Among these changes are swelling, chronic inflammation with hypervascularization, and viscous mucus due to reduced saliva production [52]. This hampers timely identification of recurrent tumors, leading to more advanced stages, and consequently diminished therapeutic options [48]. Using NBI, however, 20% more residual or recurrent tumors could be detected than with standard WLI [48]. Attention should be paid to pronounced and irregular feeding vessels, necrosis and ulceration at the mucosal surface, since normal IPCL patterns may no longer be present and classifications for untreated primary tumors (e.g. Ni's classification) are thus inapplicable [52]. Lesions were detected at an early stage (Tcis and T1) in 92% of cases, and could therefore be treated with a conservative surgical approach [48]. For NBI, 88–100% sensitivity rates were found depending on outpatient or intraoperative setting, and 92–98% specificity rates, compared to a 66% sensitivity and 100% specificity for WLI [48,52].

*Future perspectives*

With the advance of technology, further improvements with respect to endoscopy may also be expected, such as endoscopes with 4 K or even 8 K ultra-high-definition (UHD) resolution. Although this may improve the visualization of the lesion, the judgment whether a lesion is benign or malignant currently remains dependent on the observer. Classifications attempt to reduce interobserver variability and standardize diagnostics, but a computer-based diagnostic aid using artificial intelligence may be more effective in standardizing diagnostics and at the same time improve diagnostic accuracy and speed. Moreover, it could assist less experienced observers (like residents in training) new to NBI and reduce their learning curve, which is considered to be approximately 6 months [48]. Using neural networks, first attempts have been made at detecting pharyngeal and laryngeal SCC [53-55]. In a pilot study by Mascharak et al. using only 4 OPSCC lesions for training of the neural networks, a 71% sensitivity and 69% specificity for the detection of OPSCC were found, of which the sensitivity was significantly higher compared to WLI (47%) [53]. They used color and textural information of surrounding mucosa, which gave significantly better results than color information alone [53]. Addition of more image features, such as blood vessel characteristics, and a larger training dataset could possibly further increase the diagnostic accuracy of this first attempt. A neural network used by Tamashiro et al. was able to detect pharyngeal cancers, including lesions smaller than 10 mm, with an 86% sensitivity and 59% specificity for NBI, compared to a 70% sensitivity and 52% specificity for WLI [54]. Suboptimal visualization conditions such as the lesion being too distant, images showing only part of the lesion or a tangential view on the lesion hamper the diagnosis by the neural networks, and were the cause of half of the false-negative results [54]. Their system was able to analyze 50 images per second and is therefore suitable for real-time analysis [54]. Another neural network developed by Mantowski et al. was able to detect laryngeal lesions in a small set of 50 images, distinguishing papilloma/carcinoma lesions from healthy vocal cords with a 94% sensitivity and 91% specificity [55]. With improved neural networks and proper visualization of lesions during endoscopy, these first attempts hold promise for implementation of real-time assistance for the diagnosis of HNSCC in a clinical setting.

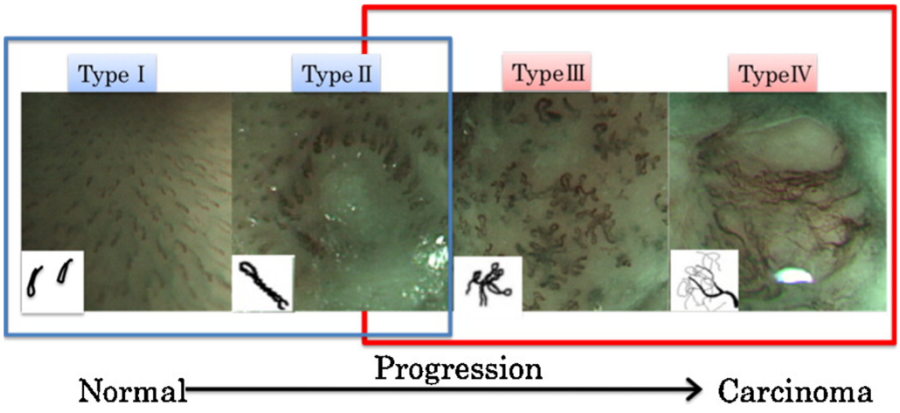


**Figure 3.** The NBI classification of oral cancer lesions as described by Takano et al. Reproduced from Takano et al., by permission of Elsevier [45].

*Optical molecular imaging using near-infrared fluorescence*

As conventional imaging techniques only reveal anatomical structures and do not offer real-time intraoperative guidance, surgeons are dependent on their own skills and judgment to decide which tissues to resect. After resection, the specimen and wound bed are inspected macroscopically, often followed by a (time-consuming) frozen section. Assessing the whole resection margin with frozen sections is generally technically not possible, thus having the risk of sampling errors. This approach leads to positive margins in 12–30% of cases [56-58]. As positive margins are associated with a poor prognosis, there is a need for improved intraoperative detection and visualization of HNSCC [59].

Fluorescent agents can be used to aid in the real-time identification of primary HNSCC. In optical image-guided surgery, the tumor-to-background ratio (TBR) is important to distinguish tumor from normal tissues [4]. Ideally, all viable tumor tissue should fluoresce, while all surrounding normal tissue should be negative for fluorescence. High sensitivity rates are required in order to remove all tumor cells, as leaving any viable tumor cells behind may have significant clinical consequences. Although a high specificity is preferable, it is of lesser importance than sensitivity, as it would not affect survival but mainly the extent of surgery.

Using relatively inexpensive and mobile cameras, optical image-guided surgery can easily be incorporated into the clinical workflow to provide real-time feedback with high imaging resolution and without exposure to ionizing radiation [19]. Moreover, fluorescence imaging may prove especially beneficial in robotic or endoscopic surgery, due to the lack of tactile feedback in these procedures [5]. Potentially, if tumors could more easily be distinguished from normal tissue, complication rates as well as operating room time can be reduced [5].

Over the past decades, fluorescence imaging has become a booming research area, with a growing number of agents and targeting strategies. Tumors may be imaged in the operating theater before or during resection (open-field), while the resected specimen can be imaged in a closed-field/back-table setting, leading to better results due to more constant imaging variables (e.g. ambient light, distance between camera and specimen).

*Untargeted near-infrared fluorescent agents*

Untargeted fluorescent agents presently include substances such as methylene blue, indocyanine green (ICG) and 5-aminolevulinic acid (ALA).

*Methylene blue* can, when sufficiently diluted, function as NIR dye emitting at around 700 nm and may be applied topically [5,19]. However, as it stains the entire surgical field and has also been overtaken by other fluorescent agents in terms of tissue penetration, it has not gained much attention [5,60].

*ICG* fluoresces at 800 nm and tumor localization can be observed as a consequence of the enhanced permeability and retention (EPR) effect that is seen in newly formed tumor tissue. In these tissues, newly formed porous blood vessels allow molecules to passively accumulate, while retention occurs due to a poorly tumor associated lymphatic system [61]. Identification and visualization of ICG may be up to 5 mm through soft tissue [62].

The use of *5-ALA* has been approved in Europe since 2007 and eventually also in the U.S. since 2017 for the use of intraoperative imaging of gliomas [63]. 5-ALA is a precursor molecule in the formation of protoporphyrin IX (PpIX). PpIX is a fluorescent molecule that mainly accumulates in gliomas, meningiomas and bladder cancer and has two emission peaks, of which one is at ~ 700 nm [5,19]. However, as it is dependent on high tumor metabolic rates, has great interindividual differences and has wavelengths with suboptimal tissue penetration, it has not been widely used outside of glioma surgery [19,64].

Overall, untargeted fluorescent agents may lead to non-specific fluorescence, higher background signals and faster clearance, reducing the time window for surgery [19]. Therefore, attempts have been made to bind fluorescent molecules to specific tumor-targeting agents for increased accuracy and efficacy.

*Targeted near-infrared fluorescent agents*

As the unbridled growth of a malignancy is associated with higher expression of growth factor receptors, angiogenesis and tumor associated metabolism, these processes form potential targets for molecular imaging [65]. Using targeted molecules can result in higher specificity and affinity, potentially lowering the required dose of the fluorescent agent and leading to better TBRs [19]. Moreover, with an increased binding time these agents could result in a prolonged time window to perform surgery, compared to ICG where peak fluorescence decreased after one hour. Targets that have been studied in HNSCC are the vascular endothelial growth factor (VEGF) receptor, epidermal growth factor receptor (EGFR), as well as tumor pH related to the Warburg effect [66]. The Warburg effect describes a change in cancer cell metabolism with higher glycolysis rates and lactate production, resulting in a lower pH. Fluorophores can be conjugated to targeting molecules, which creates fluorescent agents. Among these fluorophores, Cy5.5 and IRDye800CW have frequently been described in HNSCC [56,64,67-77]. However, as IRDye800CW has higher excitation and emission wavelengths (~790 nm) for NIR imaging than Cy5.5 (~700 nm) resulting in better tissue propagation, the former has been used most in recent studies [65].

*VEGF* is a promotor of angiogenesis and can be targeted using the antibody bevacizumab [68]. Although fluorescence could predict presence of tumor in 17 out of 18 biopsies in xenograft mouse models using bevacizumab-Cy5.5, slightly better results were found in the same mouse model using cetuximab-Cy5.5 targeting EGFR [67,68]. As bevacizumab-IRDye800CW has proven its clinical value in other types of cancer, it may be worth further studying its potential in HNSCC [78-81]. One study on the application of bevacizumab-IRDye800CW in sinonasal inverted papilloma is ongoing (NCT03925285).

*EGFR* is a transmembrane protein that is overexpressed in 90% of HNSCC and has been introduced as a target for fluorescence imaging [64,82,83]. Cetuximab is a chimeric human-murine monoclonal antibody that binds with high affinity to EGFR [83]. Several studies have used cetuximab-IRDye800CW for fluorescence imaging of HNSCC [64,70,72,77]. The TBR increased over several days after infusion, suggesting that the best moment for surgery may be 2–4 days after infusion [64]. By preloading patients with unlabeled cetuximab the highest TBRs were found, requiring lower doses of cetuximab-IRDye800CW. One study showed a feasibility of only 15 mg total dose of cetuximab-IRDye800CW conjugate for clinical use when pre-dosing was applied [70,77]. The increased TBR by preloading can be explained by the fact that antibodies accumulate more easily in normal tissue than in tumor tissue, since tumor tissue has a slower uptake as a consequence of immature vascularization and elevated interstitial pressures. Without preloading, the labeled antibodies are sequestrated in non-specific tissues, resulting in a decreased TBR [70]. In a study by Voskuil et al., all cases with a tumor-positive resection margin (<1 mm) were correctly identified at back-table fluorescence imaging of the surgical specimen directly after resection, and could assist in selecting suspect areas for fresh-frozen sections [77]. There was one false-positive case, resulting in an overall sensitivity of 100% and specificity of 91%. Moreover, in this study, one satellite tumor lesion was found, underlining the potential benefit of cetuximab-IRDye800CW in the detection of HNSCC. The use of cetuximab-IRDye800CW can be considered to be well tolerated, as there were five possibly related grade 1 adverse events out of fifteen patients [77]. Currently, a trial is ongoing studying the positive predictive value of fluorescence in margin assessment of oral cancers (NCT03134846).

Following the results found with cetuximab-IRDye800CW, several studies have been performed using panitumumab-IRDye800CW [56,69,73-76]. Panitumumab has a higher binding affinity to EGFR and improved safety profile compared to cetuximab, as it is a fully humanized monoclonal antibody [73]. An optimal dose of 50 mg

panitumumab-IRDye800CW was found to lead to the best TBRs of up to 3.6 [76]. Preloading patients with an unlabeled dose of panitumumab did not lead to additional imaging value, although it did prolong the fluorescence intensity of the labeled antibodies [76]. As with cetuximab-IRDye800CW, unanticipated second primary lesions may be detected by open-field imaging and improve surgical decision making [74]. Using closed-field analysis, TBRs of up to 6.5 were found for a dose of 50 mg panitumumab-IRDye800CW and resulted in a 100% sensitivity and 74% specificity for the detection of positive surgical margins [73]. A penetration depth of 6.3 mm was found; sufficient to detect surgical margins in HNSCC that are considered close or positive within 5 mm [56]. Back-table specimen mapping could assist in intraoperative decision making. When fluorescent hotspots are detected, this can be used to guide pathologists in taking frozen sections and thus reduce sampling errors [73]. Currently, studies are conducted in which intraoperative decision making based on the fluorescence is possible, without frozen sections. Optical analysis of an excised specimen typically takes <10 min and requires a device operator showing the data to the surgeon or pathologist.

*Future perspectives*

To further improve these results, development of new techniques can be predicted in different domains. With improved camera systems, targeting molecules with better biodistribution and binding affinity, and on-site activatable fluorescent markers, better results may be obtained.

Currently, differences in TBR are seen between open-field and closed-field imaging, in favor of the latter [73]. This is attributed to ambient light, camera angle, and distance between camera and patient affecting open-field imaging [74]. To reduce interference of ambient light, overhead lighting could be reduced or turned off. This, however, interrupts the surgical workflow [73]. New image acquisition techniques can potentially overcome this hindrance by pulsed image acquisition adjusted to the frequency of background lighting, thereby enabling subtraction of background lighting and resulting in images similar to those acquired in a completely dark room [84]. However, as orientation and interference of shadowing is especially difficult in HNSCC surgery using open-field imaging, the surgical value of fluorescence imaging may be greatest in closed-field back-table evaluation of the specimens [73].

Although results using whole antibodies such as cetuximab and panitumumab seem promising, they have a relatively large hydrodynamic diameter, resulting in accumulation in the liver, a longer bloodstream half-life, slower blood clearance and thus potentially increased background signal [5,85]. To overcome this disadvantage, smaller antigen-binding fragments have been developed such as nanobodies, which are derived from naturally occurring heavy-chain antibodies [5,85,86]. They show very specific binding and can extravasate more easily due to their small size – about one tenth of the molecular weight of monoclonal antibodies – and show rapid clearance from the body [85,86]. In a xenograft mouse model, the nanobody 7D12-IR showed optimal fluorescence contrast 2 h post-injection, compared to 24 h for cetuximab-IR. Moreover, it showed a relatively higher uptake, related to better penetration and distribution, compared to cetuximab-IR [86].

Affibody molecules are another alternative for antibodies. They are small, engineered peptides that may also bind to antibody targets [87]. Due to its rapid distribution and sufficient contrast already at 4 h after injection, it could allow for same-day surgery. Moreover, due to faster clearance, it reduces toxicity risk compared to monoclonal antibodies [87]. An Affibody trial has been completed using EGFR as a target in HNSCC and reporting of the data is expected (NCT03282461).

In addition to the currently existing fluorescent markers, quantum dots may hold promise for the future. They are small crystal nanoparticles of 2–10 nm in diameter with high signal intensity, photostability, a broad and continuous distribution of the excitation spectrum and a narrow emission spectrum that can be tuned by modifying composition and size [65,88,89]. In mice αvβ3-integrin was targeted using QD800-RGD and showed TBRs of up to 4.5 while imaging even through the skin barrier [89]. However, as the core of quantum dots is made up of heavy metals, they are potentially toxic when the cores are released [88]. Therefore, the use of quantum dots may not find their way to clinical application until quantum dots with non-toxic cores have been developed.

Another strategy of making fluorescent agents more specific, is by making them 'activatable' rather than using them in an 'always-on' state. This can be achieved by using amphiphilic polymers that form micelles in aqueous solutions and sequestrate the fluorophore, making it 'pH-activatable' and releasing the fluorophore at a certain pH threshold, as tumor is known for its acidic environment (pH <6.9) [19,66]. First in vivo results using an ultra-pH sensitive amphilic polymer conjugated to ICG (ONM-100), show a 100% sensitivity and 57% specificity for the detection of HNSCC and led to the identification of 5 occult lesions that had otherwise been missed by standard of care surgery [66].

## Conclusion

New imaging techniques have been developed for earlier and more accurate detection of HNSCC. Among these are NBI and near-infrared fluorescence imaging, which are already applied clinically and show the most potential for routine clinical use in the near future. NBI leads to improved and earlier detection of superficial mucosal HNSCC lesions compared to WLI. Future developments may enable real-time computer-assisted diagnosis during endoscopy. Near-infrared fluorescence imaging targets tumor tissue and allows for intraoperative visualization, localization and delineation of primary tumor and occult satellite lesions, and offers as main clinical advantage intraoperative margin assessment. High sensitivity and specificity rates have been found, especially when using antibody-dye conjugations. Development of better camera systems, improved targeting agents with higher affinity and biodistribution and activatable agents (e.g. pH-activatable) may further increase the future potential of near-infared fluorescence imaging. Currently, an abundance of clinical trials are being undertaken and they are expected to lead to the wide introduction of one of these compounds.

## Declaration of Competing Interest

Boudewijn E.C. Plaat has a consultancy role for and has received unrestricted research grants from Olympus Medical Systems EU. The authors have no other funding, financial relationships, or conflicts of interest to disclose.

## References

[1] Schutte HW, Heutink F, Wellenstein DJ, van den Broek GB, van den Hoogen FJA, Marres HAM, et al. Impact of Time to Diagnosis and Treatment in Head and Neck Cancer: A Systematic Review. Otolaryngol Head Neck Surg. 2020;162:446–57. https://doi.org/10.1177/0194599820906387.

[2] Kain JJ, Birkeland AC, Udayakumar N, Morlandt AB, Stevens TM, Carroll WR, et al. Surgical margins in oral cavity squamous cell carcinoma: Current practices and future directions. Laryngoscope. 2020;130:128–38. https://doi.org/10.1002/lary.27943.

[3] Lauwerends LJ, Galema HA, Hardillo JAU, Sewnaik A, Monserez D, van Driel PBAA, et al. Current Intraoperative Imaging Techniques to Improve Surgical Resection of Laryngeal Cancer: A Systematic Review. Cancers (Basel). 2021;13:1895. https://doi.org/10.3390/cancers13081895.

[4] Keereweer S, Kerrebijn JDF, Mol IM, Mieog JSD, Van Driel PBAA, Baatenburg de Jong RJ, et al. Optical imaging of oral squamous cell carcinoma and cervical lymph node metastasis. Head Neck. 2012;34:1002–8. https://doi.org/10.1002/hed.21861.

[5] Vahrmeijer AL, Hutteman M, van der Vorst JR, van de Velde CJH, Frangioni JV. Image-guided cancer surgery using near-infrared fluorescence. Nat Rev Clin Oncol. 2013;10:507–18. https://doi.org/10.1038/nrclinonc.2013.123.

[6] Muto M, Hironaka S, Nakane M, Boku N, Ohtsu A, Yoshida S. Association of multiple Lugol-voiding lesions with synchronous and metachronous esophageal squamous cell carcinoma in patients with head and neck cancer. Gastrointest Endosc. 2002;56:517–21. https://doi.org/10.1016/S0016-5107(02)70436-7.

[7] Epstein JB, Scully C, Spinelli J. Toluidine blue and Lugol's iodine application in the assessment of oral malignant disease and lesions at risk of malignancy. J Oral

Pathol Med. 1992;21:160–3. https://doi.org/10.1111/j.1600-0714.1992.tb00094.x.
[8] McMahon J, Devine JC, McCaul JA, McLellan DR, Farrow A. Use of Lugol's iodine in the resection of oral and oropharyngeal squamous cell carcinoma. Br J Oral Maxillofac Surg. 2009;48:84–7. https://doi.org/10.1016/j.bjoms.2009.05.007.
[9] Nonaka S, Saito Y. Endoscopic diagnosis of pharyngeal carcinoma by NBI. Endoscopy. 2008;40:347–51. https://doi.org/10.1055/s-2007-995433.
[10] Sridharan G, Shankar AA. Toluidine blue: A review of its chemistry and clinical utility. J Oral Maxillofac Pathol. 2012;16:251–5. https://doi.org/10.4103/0973-029X.99081.
[11] Kim DH, Kim SW, Hwang SH. Autofluorescence imaging to identify oral malignant or premalignant lesions: Systematic review and meta-analysis. Head Neck. 2020;42:3735–43. https://doi.org/10.1002/hed.26430.
[12] Tarabichi O, Bulbul MG, Kanumuri VV, Faquin WC, Juliano AF, Cunnane ME, et al. Utility of intraoral ultrasound in managing oral tongue squamous cell carcinoma: Systematic review. Laryngoscope. 2019;129:662–70. https://doi.org/10.1002/lary.27403.
[13] Hatta W, Uno K, Koike T, Yokosawa S, Iijima K, Imatani A, et al. Optical coherence tomography for the staging of tumor infiltration in superficial esophageal squamous cell carcinoma. Gastrointest Endosc. 2010;71:899–906. https://doi.org/10.1016/j.gie.2009.11.052.
[14] De Leeuw F, Abbaci M, Casiraghi O, Ben Lakhdar A, Alfaro A, Breuskin I, et al. Value of Full-Field Optical Coherence Tomography Imaging for the Histological Assessment of Head and Neck Cancer. Lasers Surg Med. 2020. https://doi.org/10.1002/lsm.23223.
[15] Volgger V, Stepp H, Ihrler S, Kraft M, Leunig A, Patel PM, et al. Evaluation of optical coherence tomography to discriminate lesions of the upper aerodigestive tract. Head Neck. 2013;35:1558–66. https://doi.org/10.1002/hed.23189.
[16] Hamdoon Z, Jerjes W, McKenzie G, Jay A, Hopper C. Optical coherence tomography in the assessment of oral squamous cell carcinoma resection margins. Photodiagnosis Photodyn Ther. 2015;13:211–7. https://doi.org/10.1016/j.pdpdt.2015.07.170.
[17] Wang J, Xu Y, Boppart SA. Review of optical coherence tomography in oncology. J Biomed Opt. 2017;22:1–23. https://doi.org/10.1117/1.JBO.22.12.121711.
[18] Sunny SP, Agarwal S, James BL, Heidari E, Muralidharan A, Yadav V, et al. Intra-operative point-of-procedure delineation of oral cancer margins using optical coherence tomography. Oral Oncol. 2019;92:12–9. https://doi.org/10.1016/j.oraloncology.2019.03.006.
[19] Wang C, Wang Z, Zhao T, Li Y, Huang G, Sumer BD, et al. Optical molecular imaging for tumor detection and image-guided surgery. Biomaterials 2018;157:62–75. https://doi.org/10.1016/j.biomaterials.2017.12.002.
[20] Kraft M, Betz CS, Leunig A, Arens C. Value of fluorescence endoscopy for the early diagnosis of laryngeal cancer and its precursor lesions. Head Neck. 2011;33:941–8. https://doi.org/10.1002/hed.21565.
[21] Keereweer S, Sterenborg HJCM, Kerrebijn JDF, Van Driel PBAA, Baatenburg de Jong RJ, Löwik CWGM. Image-guided surgery in head and neck cancer: Current practice and future directions of optical imaging. Head Neck. 2012;34:120–6. https://doi.org/10.1002/hed.21625.
[22] Sweeny L, Dean NR, Magnuson JS, Carroll WR, Clemons L, Rosenthal EL. Assessment of Tissue Autofluorescence and Reflectance for Oral Cavity Cancer Screening. Otolaryngol Head Neck Surg. 2011;145:956–60. https://doi.org/10.1177/0194599811416773.
[23] Harris AT, Rennie A, Waqar-Uddin H, Wheatley SR, Ghosh SK, Martin-Hirsch DP, et al. Raman spectroscopy in head and neck cancer. Head Neck Oncol. 2010;2:26. https://doi.org/10.1186/1758-3284-2-26.
[24] Guze K, Pawluk HC, Short M, Zeng H, Lorch J, Norris C, et al. Pilot study: Raman spectroscopy in differentiating premalignant and malignant oral lesions from normal mucosa and benign lesions in humans. Head Neck. 2015;37:511–7. https://doi.org/10.1002/hed.23629.
[25] Stone N, Stavroulaki P, Kendall C, Birchall M, Barr H. Raman Spectroscopy for Early Detection of Laryngeal Malignancy: Preliminary Results. Laryngoscope. 2000;110:1756–63. https://doi.org/10.1097/00005537-200010000-00037.
[26] Barroso EM, Smits RWH, Bakker Schut TC, ten Hove I, Hardillo JA, Wolvius EB, et al. Discrimination between Oral Cancer and Healthy Tissue Based on Water Content Determined by Raman Spectroscopy. Anal Chem. 2015;87:2419–26. https://doi.org/10.1021/ac504362y.
[27] Wu C, Gleysteen J, Teraphongphom NT, Li Y, Rosenthal E. In-vivo optical imaging in head and neck oncology: basic principles, clinical applications and future directions. Int J Oral Sci. 2018;10:10–3. https://doi.org/10.1038/s41368-018-0011-4.
[28] Santos IP, Barroso EM, Bakker Schut TC, Caspers PJ, van Lanschot CGF, Choi D, et al. Raman spectroscopy for cancer detection and cancer surgery guidance: translation to the clinics. Analyst. 2017;142:3025–47. https://doi.org/10.1039/c7an00957g.
[29] Kumagai Y, Toi M, Inoue H. Dynamism of tumour vasculature in the early phase of cancer progression: outcomes from oesophageal cancer research. Lancet Oncol. 2002;3:604–10. https://doi.org/10.1016/s1470-2045(02)00874-4.
[30] Ni X, He S, Xu Z, Gao L, Lu N, Yuan Z, et al. Endoscopic diagnosis of laryngeal cancer and precancerous lesions by narrow band imaging. J Laryngol Otol. 2011;125:288–96. https://doi.org/10.1017/S0022215110002033.
[31] Gono K, Obi T, Yamaguchi M, Ohyama N, Machida H, Sano Y, et al. Appearance of enhanced tissue features in narrow-band endoscopic imaging. J Biomed Opt. 2004;9:568–77. https://doi.org/10.1117/1.1695563.
[32] Vu AN, Farah CS. Efficacy of narrow band imaging for detection and surveillance of potentially malignant and malignant lesions in the oral cavity and oropharynx: A systematic review. Oral Oncol. 2014;50:413–20. https://doi.org/10.1016/j.oraloncology.2014.02.002.
[33] Cosway B, Drinnan M, Paleri V. Narrow band imaging for the diagnosis of head and neck squamous cell carcinoma: A systematic review. Head Neck. 2016;38:E2358–67. https://doi.org/10.1002/hed.24300.
[34] Zhou H, Zhang J, Guo L, Nie J, Zhu C, Ma X. The value of narrow band imaging in diagnosis of head and neck cancer: a meta-analysis. Sci Rep. 2018;8:515. https://doi.org/10.1038/s41598-017-19069-0.
[35] Chu EA, Kim YJ. Laryngeal Cancer: Diagnosis and Preoperative Work-up. Otolaryngol Clin North Am. 2008;41:673–95. https://doi.org/10.1016/j.otc.2008.01.016.
[36] Kraft M, Fostiropoulos K, Gürtler N, Arnoux A, Davaris N, Arens C. Value of narrow band imaging in the early diagnosis of laryngeal cancer. Head Neck. 2016;38:15–20. https://doi.org/10.1002/hed.23838.
[37] Mehlum CS, Rosenberg T, Dyrvig A, Groentved AM, Kjaergaard T, Godballe C. Can the Ni classification of vessels predict neoplasia? A systematic review and meta-analysis. Laryngoscope. 2018;128:168–76. https://doi.org/10.1002/lary.26721.
[38] Arens C, Piazza C, Anea M, Dikkers FG, Tjon Pian Gi RE, Voigt-Zimmermann S, et al. Proposal for a descriptive guideline of vascular changes in lesions of the vocal folds by the committee on endoscopic laryngeal imaging of the European Laryngological Society. Eur Arch Otorhinolaryngol. 2016;273:1207–14. https://doi.org/10.1007/s00405-015-3851-y.
[39] Kim DH, Kim Y, Kim SW, Hwang SH. Use of narrowband imaging for the diagnosis and screening of laryngeal cancer: A systematic review and meta-analysis. Head Neck. 2020. https://doi.org/10.1002/hed.26186.
[40] Zwakenberg MA, Dikkers FG, Wedman J, Halmos GB, van der Laan BFAM, Plaat BE. Narrow band imaging improves observer reliability in evaluation of upper aerodigestive tract lesions. The Laryngoscope. 2016;126:2276–81. https://doi.org/10.1002/lary.26008.
[41] Zwakenberg MA, Dikkers FG, Wedman J, van der Laan BFAM, Halmos GB, Plaat BEC. Detection of high-grade dysplasia, carcinoma in situ and squamous cell carcinoma in the upper aerodigestive tract: Recommendations for optimal use and interpretation of narrow-band imaging. Clin Otolaryngol. 2019;44:39–46. https://doi.org/10.1111/coa.13229.
[42] Zwakenberg MA, Plaat BEC. A Photographic Atlas of Lesions in the Pharynx and Larynx: Conventional White Light Imaging versus Narrow Band Imaging. ISBN/EAN: 978-90-9032253-7. Hamburg: Olympus Europe SE & CO. KG.; 2019.
[43] Lin Y, Wang W, Lee K, Tsai W, Weng H. Value of narrow band imaging endoscopy in early mucosal head and neck cancer. Head Neck. 2012;34:1574–9. https://doi.org/10.1002/hed.21964.
[44] Piazza C, Del Bon F, Paderno A, Grazioli P, Perotti P, Barbieri D, et al. The diagnostic value of narrow band imaging in different oral and oropharyngeal subsites. Eur Arch Otorhinolaryngol. 2016;273:3347–53. https://doi.org/10.1007/s00405-016-3925-5.
[45] Takano JH, Yakushiji T, Kamiyama I, Nomura T, Katakura A, Takano N, et al. Detecting early oral cancer: narrowband imaging system observation of the oral mucosa microvasculature. Int J Oral Maxillofac Surg. 2010;39:208–13. https://doi.org/10.1016/j.ijom.2010.01.007.
[46] Yang S, Lee Y, Chang L, Hwang C, Chen T. Diagnostic significance of narrow-band imaging for detecting high-grade dysplasia, carcinoma in situ, and carcinoma in oral leukoplakia. Laryngoscope. 2012;122:2754–61. https://doi.org/10.1002/lary.23629.
[47] Ansari UH, Wong E, Smith M, Singh N, Palme CE, Smith MC, et al. Validity of narrow band imaging in the detection of oral and oropharyngeal malignant lesions: A systematic review and meta-analysis. Head Neck. 2019;41:2430–40. https://doi.org/10.1002/hed.25724.
[48] Piazza C, Cocco D, De Benedetto L, Bon FD, Nicolai P, Peretti G. Role of narrow-band imaging and high-definition television in the surveillance of head and neck squamous cell cancer after chemo- and/or radiotherapy. Eur Arch Otorhinolaryngol. 2010;267:1423–8. https://doi.org/10.1007/s00405-010-1236-9.
[49] Zhu L, Wang N. 18F-fluorodeoxyglucose positron emission tomography-computed tomography as a diagnostic tool in patients with cervical nodal metastases of unknown primary site: A meta-analysis. Surg Oncol. 2013;22:190–4. https://doi.org/10.1016/j.suronc.2013.06.002.
[50] Fu TS, Foreman A, Goldstein DP, de Almeida JR. The role of transoral robotic surgery, transoral laser microsurgery, and lingual tonsillectomy in the identification of head and neck squamous cell carcinoma of unknown primary origin: a systematic review. J Otolaryngol Head Neck Surg. 2016;45:28. https://doi.org/10.1186/s40463-016-0142-6.
[51] Filauro M, Paderno A, Perotti P, Marchi F, Garofolo S, Peretti G, et al. Role of narrow-band imaging in detection of head and neck unknown primary squamous cell carcinoma. Laryngoscope. 2018;128:2060–6. https://doi.org/10.1002/lary.27098.
[52] Zabrodsky M, Lukes P, Lukesova E, Boucek J, Plzak J. The Role of Narrow Band Imaging in the Detection of Recurrent Laryngeal and Hypopharyngeal Cancer after Curative Radiotherapy. Biomed Res Int. 2014;2014:175398–9. https://doi.org/10.1155/2014/175398.
[53] Mascharak S, Baird BJ, Holsinger FC. Detecting oropharyngeal carcinoma using multispectral, narrow-band imaging and machine learning. Laryngoscope. 2018;128:2514–20. https://doi.org/10.1002/lary.27159.
[54] Tamashiro A, Yoshio T, Ishiyama A, Tsuchida T, Hijikata K, Yoshimizu S, et al. Artificial intelligence-based detection of pharyngeal cancer using convolutional neural networks. Dig Endosc. 2020. https://doi.org/10.1111/den.13653.

[55] Mantowski S, Volgger V, Schuster M, Lohscheller J. Computer-assisted classification of vocal fold diseases lesions on NBI images using deep convolutional neural networks. SPIE Conference 2018;10469:10469–511.

[56] Van Keulen S, Van den Berg NS, Nishio N, Birkeland A, Zhou Q, Lu G, et al. Rapid, non-invasive fluorescence margin assessment: Optical specimen mapping in oral squamous cell carcinoma. Oral Oncol. 2019;88:58–65. https://doi.org/10.1016/j.oraloncology.2018.11.012.

[57] Wong LS, McMahon J, Devine J, McLellan D, Thompson E, Farrow A, et al. Influence of close resection margins on local recurrence and disease-specific survival in oral and oropharyngeal carcinoma. Br J Oral Maxillofac Surg. 2011;50:102–8. https://doi.org/10.1016/j.bjoms.2011.05.008.

[58] Woolgar JA, Triantafyllou A. A histopathological appraisal of surgical margins in oral and oropharyngeal cancer resection specimens. Oral Oncol. 2005;41:1034–43. https://doi.org/10.1016/j.oraloncology.2005.06.008.

[59] Hinni ML, Ferlito A, Brandwein-Gensler MS, Takes RP, Silver CE, Westra WH, et al. Surgical margins in head and neck cancer: A contemporary review. Head Neck. 2013;35:1362–70. https://doi.org/10.1002/hed.23110.

[60] van der Vorst JR, Schaafsma BE, Verbeek FPR, Keereweer S, Jansen JC, van der Velden L, et al. Near-infrared fluorescence sentinel lymph node mapping of the oral cavity in head and neck cancer patients. Oral Oncol. 2012;49:15–9. https://doi.org/10.1016/j.oraloncology.2012.07.017.

[61] Schaafsma BE, Mieog JSD, Hutteman M, van der Vorst JR, Kuppen PJK, Löwik CWGM, et al. The clinical use of indocyanine green as a near-infrared fluorescent contrast agent for image-guided oncologic surgery. J Surg Oncol. 2011;104:323–32. https://doi.org/10.1002/jso.21943.

[62] Bredell MG. Sentinel lymph node mapping by indocyanin green fluorescence imaging in oropharyngeal cancer - preliminary experience. Head Neck Oncol. 2010;2:31. https://doi.org/10.1186/1758-3284-2-31.

[63] Hadjipanayis CG, Stummer W. 5-ALA and FDA approval for glioma surgery. J Neurooncol. 2019;141:479–86. https://doi.org/10.1007/s11060-019-03098-y.

[64] Rosenthal EL, Warram JM, de Boer E, Chung TK, Korb ML, Brandwein-Gensler M, et al. Safety and Tumor Specificity of Cetuximab-IRDye800 for Surgical Navigation in Head and Neck Cancer. Clin Cancer Res 2015;21:3658–66. https://doi.org/10.1158/1078-0432.CCR-14-3284.

[65] Yokoyama J, Fujimaki M, Ohba S, Anzai T, Yoshii R, Ito S, et al. A feasibility study of NIR fluorescent image-guided surgery in head and neck cancer based on the assessment of optimum surgical time as revealed through dynamic imaging. Onco Targets Ther. 2013;6:325–30. https://doi.org/10.2147/OTT.S42006.

[66] Voskuil FJ, Steinkamp PJ, Zhao T, van der Vegt B, Koller M, Doff JJ, et al. Exploiting metabolic acidosis in solid cancers using a tumor-agnostic pH-activatable nanoprobe for fluorescence-guided surgery. Nat Commun. 2020;11:3257. https://doi.org/10.1038/s41467-020-16814-4.

[67] Rosenthal EL, Kulbersh BD, Duncan RD, Zhang W, Magnuson JS, Carroll WR, et al. In Vivo Detection of Head and Neck Cancer Orthotopic Xenografts by Immunofluorescence. Laryngoscope. 2006;116:1636–41. https://doi.org/10.1097/01.mlg.0000232513.19873.da.

[68] Withrow KP, Newman JR, Skipper JB, Gleysteen JP, Magnuson JS, Zinn K, et al. Assessment of Bevacizumab Conjugated to Cy5.5 for Detection of Head and Neck Cancer Xenografts. Technol Cancer Res Treat. 2008;7:61–6. https://doi.org/10.1177/153303460800700108.

[69] Heath CH, Deep NL, Sweeny L, Zinn KR, Rosenthal EL. Use of Panitumumab-IRDye800 to Image Microscopic Head and Neck Cancer in an Orthotopic Surgical Model. Ann Surg Oncol. 2012;19:3879–87. https://doi.org/10.1245/s10434-012-2435-y.

[70] Moore LS, Rosenthal EL, de Boer E, Prince AC, Patel N, Richman JM, et al. Effects of an Unlabeled Loading Dose on Tumor-Specific Uptake of a Fluorescently Labeled Antibody for Optical Surgical Navigation. Mol Imaging Biol. 2017;19:610–6. https://doi.org/10.1007/s11307-016-1022-1.

[71] Moore LS, Rosenthal EL, Chung TK, de Boer E, Patel N, Prince AC, et al. Characterizing the Utility and Limitations of Repurposing an Open-Field Optical Imaging Device for Fluorescence-Guided Surgery in Head and Neck Cancer Patients. J Nucl Med. 2017;58:246–51. https://doi.org/10.2967/jnumed.115.171413.

[72] Rosenthal EL, Moore LS, Tipirneni K, de Boer E, Stevens TM, Hartman YE, et al. Sensitivity and Specificity of Cetuximab-IRDye800CW to Identify Regional Metastatic Disease in Head and Neck Cancer. Clin Cancer Res 2017;23:4744–52. https://doi.org/10.1158/1078-0432.CCR-16-2968.

[73] Gao RW, Teraphongphom NT, van den Berg NS, Martin BA, Oberhelman NJ, Divi V, et al. Determination of Tumor Margins with Surgical Specimen Mapping Using Near-Infrared Fluorescence. Cancer Res. 2018;78:5144–54. https://doi.org/10.1158/0008-5472.CAN-18-0878.

[74] van Keulen S, Nishio N, Fakurnejad S, Birkeland A, Martin BA, Lu G, et al. The clinical application of fluorescence-guided surgery in head and neck cancer. J Nucl Med. 2019;60:758–63. https://doi.org/10.2967/jnumed.118.222810.

[75] Nishio N, van den Berg NS, van Keulen S, Martin BA, Fakurnejad S, Teraphongphom N, et al. Optical molecular imaging can differentiate metastatic from benign lymph nodes in head and neck cancer. Nat Commun. 2019;10:1–10. https://doi.org/10.1038/s41467-019-13076-7.

[76] Nishio N, van den Berg NS, van Keulen S, Martin BA, Fakurnejad S, Zhou Q, et al. Optimal Dosing Strategy for Fluorescence-Guided Surgery with Panitumumab-IRDye800CW in Head and Neck Cancer. Mol Imaging Biol. 2020;22:156–64. https://doi.org/10.1007/s11307-019-01358-x.

[77] Voskuil FJ, de Jongh SJ, Hooghiemstra WTR, Linssen MD, Steinkamp PJ, de Visscher SAHJ, et al. Fluorescence-guided imaging for resection margin evaluation in head and neck cancer patients using cetuximab-800CW: A quantitative dose-escalation study. Theranostics. 2020;10:3994–4005. https://doi.org/10.7150/thno.43227.

[78] Steinkamp PJ, Pranger BK, Li M, Linssen MD, Voskuil FJ, Been LB, et al. Fluorescence-guided visualization of soft tissue sarcomas by targeting vascular endothelial growth factor-A: a phase 1 single-center clinical trial. J Nucl Med. 2020;120:245696. https://doi.org/10.2967/jnumed.120.245696.

[79] Koller M, Qiu S, Linssen MD, Jansen L, Kelder W, de Vries J, et al. Implementation and benchmarking of a novel analytical framework to clinically evaluate tumor-specific fluorescent tracers. Nat Commun. 2018;9:3739–811. https://doi.org/10.1038/s41467-018-05727-y.

[80] Harlaar NJ, Koller M, de Jongh SJ, van Leeuwen BL, Hemmer PH, Kruijff S, et al. Molecular fluorescence-guided surgery of peritoneal carcinomatosis of colorectal origin: a single-centre feasibility study. Lancet Gastroenterol Hepatol. 2016;1:283–90. https://doi.org/10.1016/S2468-1253(16)30082-6.

[81] Hartmans E, Tjalma JJJ, Linssen MD, Allende PBG, Koller M, Jorritsma-Smit A, et al. Potential Red-Flag Identification of Colorectal Adenomas with Wide-Field Fluorescence Molecular Endoscopy. 2018;8:1458–67. https://doi.org/10.7150/thno.22033.

[82] Grandis JR, Melhem MF, Gooding WE, Day R, Holst VA, Wagener MM, et al. Levels of TGF-α and EGFR Protein in Head and Neck Squamous Cell Carcinoma and Patient Survival. J Natl Cancer Inst. 1998;90:824–32. https://doi.org/10.1093/jnci/90.11.824.

[83] Harding J, Burtness B. Cetuximab: An epidermal growth factor receptor chimeric human-murine monoclonal antibody. Drugs Today (Barc). 2005;41:107. https://doi.org/10.1358/dot.2005.41.2.882662.

[84] Sexton KJ, Zhao Y, Davis SC, Jiang S, Pogue BW. Optimization of fluorescent imaging in the operating room through pulsed acquisition and gating to ambient background cycling. Biomed Opt Express. 2017;8:2635–48. https://doi.org/10.1364/BOE.8.002635.

[85] Van Driel PBAA, Van Der Vorst JR, Verbeek FPR, Oliveira S, Snoeks TJA, Keereweer S, et al. Intraoperative fluorescence delineation of head and neck cancer with a fluorescent Anti-epidermal growth factor receptor nanobody. Int J Cancer. 2014;134:2663–73. https://doi.org/10.1002/ijc.28601.

[86] Oliveira S, van Dongen GAMS, Stigter-van Walsum M, Roovers RC, Stam JC, Mali W, et al. Rapid Visualization of Human Tumor Xenografts through Optical Imaging with a Near-infrared Fluorescent Anti-Epidermal Growth Factor Receptor Nanobody. Mol Imaging. 2012;11:33–46. https://doi.org/10.2310/7290.2011.00025.

[87] Samkoe KS, Sardar HS, Bates BD, Tselepidakis NN, Gunn JR, Hoffer-Hawlik KA, et al. Preclinical imaging of epidermal growth factor receptor with ABY-029 in soft-tissue sarcoma for fluorescence-guided surgery and tumor detection. J Surg Oncol. 2019;119:1077–86. https://doi.org/10.1002/jso.25468.

[88] Yang K, Zhao C, Cao Y, Tang H, Bai Y, Huang H, et al. In vivo and in situ imaging of head and neck squamous cell carcinoma using near-infrared fluorescent quantum dot probes conjugated with epidermal growth factor receptor monoclonal antibodies in mice. Oncol Rep. 2012;27:1925–31. https://doi.org/10.3892/or.2012.1705.

[89] Huang H, Bai Y, Yang K, Tang H, Wang Y. Optical imaging of head and neck squamous cell carcinoma in vivo using arginine-glycine- aspartic acid peptide conjugated near-infrared quantum dots. Onco Targets Ther. 2013;6:1779–87. https://doi.org/10.2147/OTT.S53901.

[90] Schmidt F, Dittberner A, Koscielny S, Petersen I, Guntinas-Lichius O. Feasibility of real-time near-infrared indocyanine green fluorescence endoscopy for the evaluation of mucosal head and neck lesions. Head Neck 2017;39:234–40. https://doi.org/10.1002/hed.24570.

[91] Huang T, Huang J, Wang Y, Chen K, Wong T, Chen Y, et al. Novel quantitative analysis of autofluorescence images for oral cancer screening. Oral Oncol 2017;68:20–6. https://doi.org/10.1016/j.oraloncology.2017.03.003.

[92] Huang T, Chen K, Wong T, Chen C, Chen W, Chen Y, et al. Two-channel autofluorescence analysis for oral cancer. J Biomed Opt 2018;24:1–10. https://doi.org/10.1117/1.JBO.24.5.051402.

[93] Cals FLJ, Bakker Schut TC, Caspers PJ, Baatenburg de Jong RJ, Koljenovi S, Puppels GJ. Raman spectroscopic analysis of the molecular composition of oral cavity squamous cell carcinoma and healthy tongue tissue. Analyst. 2018;143:4090–102. https://doi.org/10.1039/c7an02106b.

[94] Pujary P, Maheedhar K, Krishna CM, Pujary K. Raman Spectroscopic Methods for Classification of Normal and Malignant Hypopharyngeal Tissues: An Exploratory Study. Pathology research international. 2011;2011:632493–9. https://doi.org/10.4061/2011/632493.

[95] Englhard AS, Betz T, Volgger V, Lankenau E, Ledderose GJ, Stepp H, et al. Intraoperative assessment of laryngeal pathologies with optical coherence tomography integrated into a surgical microscope. Lasers Surg Med 2017;49:490–7. https://doi.org/10.1002/lsm.22632.

[96] Just T, Lankenau E, Prall F, Hüttmann G, Pau HW, Sommer K. Optical coherence tomography allows for the reliable identification of laryngeal epithelial dysplasia and for precise biopsy: A clinicopathological study of 61 patients undergoing microlaryngoscopy. The Laryngoscope. 2010;120:1964–70. https://doi.org/10.1002/lary.21057.

[97] Lloyd GR, Orr LE, Christie-Brown J, McCarthy K, Rose S, Thomas M, et al. Discrimination between benign, primary and secondary malignancies in lymph nodes from the head and neck utilising Raman spectroscopy and multivariate analysis. Analyst. 2013;138:3900–8. https://doi.org/10.1039/c2an36579k.

[98] Website: https://www.olympus-global.com/en/news/2011a/image/nr110526awarde_01.jpg, last accessed on 11 June 2021.